<u>Additional File 1.</u> Supplementary material for the article.

Table S1. *S. cerevisiae* strains used in this study. All strains are derived from W303 strain 1002 (*MAT*α, *ade2-1, trp1-1, can1-100, leu2-3,112, his3-11,15, ura3*) unless stated otherwise.

Strain	Genotype	Usage
YMAA1	Delta-integration of P_{TEF1}-NpR5600-T_{CYC1}-P_{TEF1}-NpR5599- T_{CYC1}-HYG and P_{TEF1}-NpR5598- T_{CYC1}- P_{TEF1}-NpR5597- T_{CYC1}-NAT into W303 (MATα)	Figure 1B
YMAA2	YMAA1 *tal1::HIS3MX6*	Figure 1G
YMAA3	YMAA1 *pfk2::KANMX6*	Figure 2B
YMAA4	YMAA1 *tkl2::KANMX6*	Figure S3
YMAA5	YMAA1 *tkl1::KANMX6*	Figure S3
YMAA6	YMAA1 *pfk2::KANMX6 zwf1::HIS3MX6*	Figure 3B
YMAA7	YMAA1 *zwf1::HIS3MX6*	Figure 1C
YMAA8	YMAA1 *pfk2::KANMX6 tal1::HIS3MX6*	Figure 2E
YMAA9	YMAA1 *tkl1::KANMX6 tkl2::HIS3MX6*	Figure 1E
YMAA10	YMAA1 *pho13::HIS3MX6*	Figure S5
YMAA11	YMAA1 *nqm1::HIS3MX6*	Figure S4
YMAA12	YMAA1 *pfk1::HIS3MX6*	Figure 2C
YMAA13	YMAA1 *shb17::KANMX6*	Figure S5

YMAA15	YMAA1 *pfk2::KANMX6 nqm1::HIS3MX6*	Figure S4
YMAA23	YMAA3 harbouring wild type *PFK2* in pFL38 (expression vector containing *URA3* marker)PFK2	Figure S6
YMAA24	YMAA3 harbouring PFK2 D309T in pFL38 (expression vector containing *URA3* marker)	Figure S6
YMAA25	YMAA3 harbouring PFK2 D356S in pFL38 (expression vector containing *URA3* marker)	Figure S6
YMAA26	YMAA3 harbouring PFK2 R447S in pFL38 (expression vector containing *URA3* marker)	Figure S6
YMAA27	YMAA3 harbouring PFK2 H488S in pFL38 (expression vector containing *URA3* marker)	Figure S6
YMAA28	YMAA3 harbouring EcPFKA in pRS316 (2-micron vector containing *URA3* marker)EcPFKa	Figure S6
YMAA29	YMAA3 harbouring empty pRS316 (2-micron vector containing *URA3* marker)vector	Figure S6
YMAA30	YMAA1 *pfk2::KANMX6 prm15::HIS3MX6*	Figure S7
YMAA31	YMAA1 *pfk2::KANMX6 urh1::HIS3MX6*	Figure S7
YMAA32	YMAA1 *pnp1::HIS3MX6*	Figure S7
YMAA33	YMAA1 *prm15::HIS3MX6*	Figure S7

YMAA34	YMAA1 *atg1::HIS3MX6*	Figure S7
YMAA35	YMAA1 *urh1::HIS3MX6*	Figure S7
YMAA36	YMAA1 *pfk2::KANMX6 atg1::HIS3MX6*	Figure S7
YMAA37	YMAA1 *pfk2::KANMX6*, *tkl1::HIS3MX6, tkl2::HIS3MX6* (generated by crossing)	Figure 3D
YMAA38	YMAA1 P_{TEF1}-TKL1	Figure S10
YMAA39	YMAA1 P_{TEF1}-TKL2	Figure S10
YMAA40	YMAA1 *pfk2::KANMX6 pnp1::HIS3MX6*	Figure S7
YMAA41	YMAA1 *pfk2::KANMX6 atg7::HIS3MX6*	Figure S7
YMAA42	YMAA1 *aro1::HIS3MX6*	Figure 1C
YMAA43	YMAA1 *tal1::HIS3MX6*, *nqm1::HIS3MX6*	Figure S4
YMAA45	MAT-a YMAA1 *pfk2::KANMX6 tal1:HIS3MX6, nqm1::HIS3MX6*	Figure S4
YMAA49	*tal1::HIS3MX6*	Figure 2C
YMAA50	*pfk1::HIS3MX6*	Figure 2C
YMAA51	YMAA1 *pfk2::KANMX6 pfk1::HIS3MX6*	Figure 4C
YMAA54	*zwf1::HIS3MX6*	Figure 1D
YMAA55	*tkl1::HIS3MX6 tkl2::KANMX6*	Figure 1D

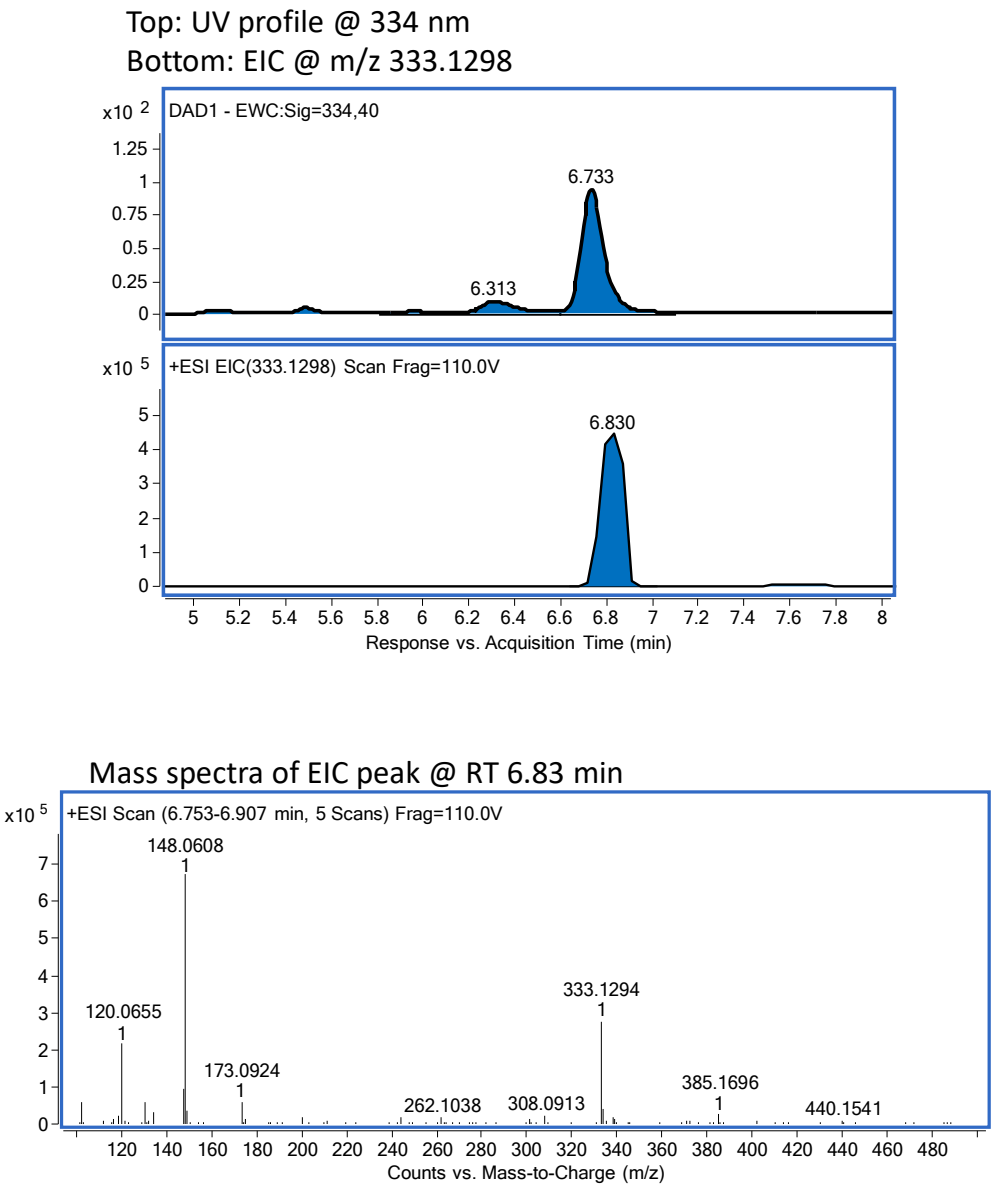

Figure S1. (Top panel) The UV absorption profile of the shinorine-producing strain's extract at 334 nm. (Bottom panel) The mass spectrum of the EIC peak detected at RT 6.83 min.

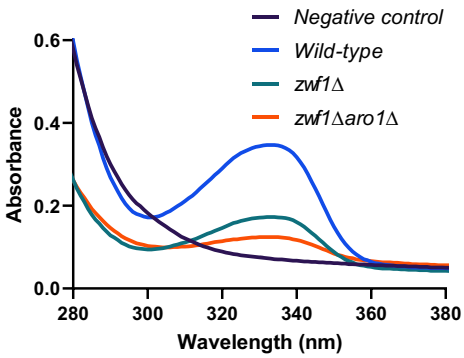

Figure S2. The UV absorption profiles of the wild-type, *zwf1Δ*, and *zwf1Δaro1Δ* strains.

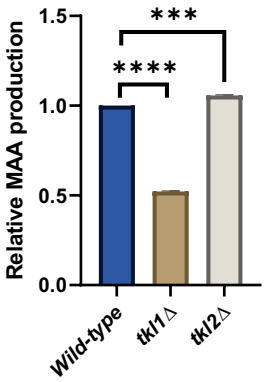

Figure S3. Comparison of shinorine levels in the wild-type, *tkl1*Δ and *tkl2*Δ strains.

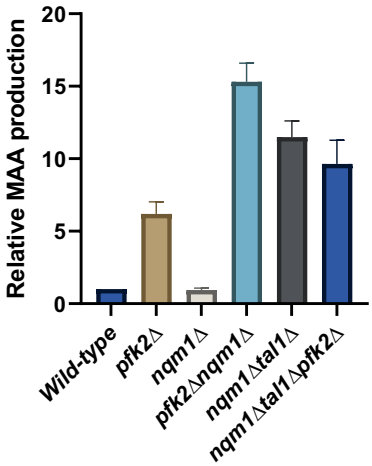

Figure S4. Comparison of shinorine levels in the wild-type, *pfk2*Δ, *nqm1*Δ, *pfk2*Δ*nqm1*Δ, *nqm1*Δ*tal1*Δ and *nqm1*Δ *tal1*Δ *pfk2*Δ strains.

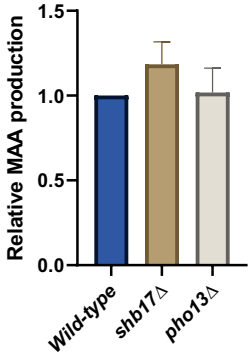

Figure S5. Comparison of shinorine levels in the wild-type, *shb17*Δ and *pho13*Δ strains.

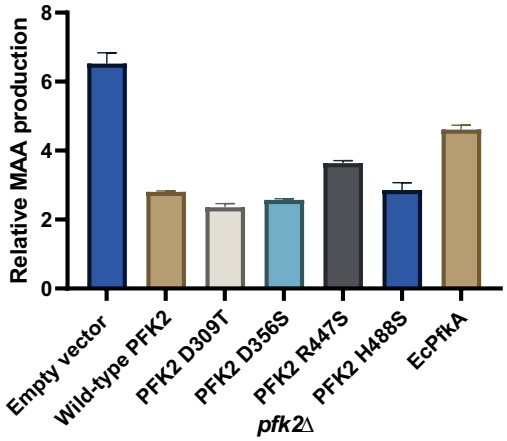

Figure S6. Comparison of shinorine levels produced in the *pfk2Δ* strains harbouring vectors with *PFK* variants.

Table S2. A description of the roles of *PFK2* mutations tested.

Mutation	Effect
D309T	ATP binding
D356S	Substrate binding
R447S	Effector PEP/ADP binding
H488S	Substrate binding

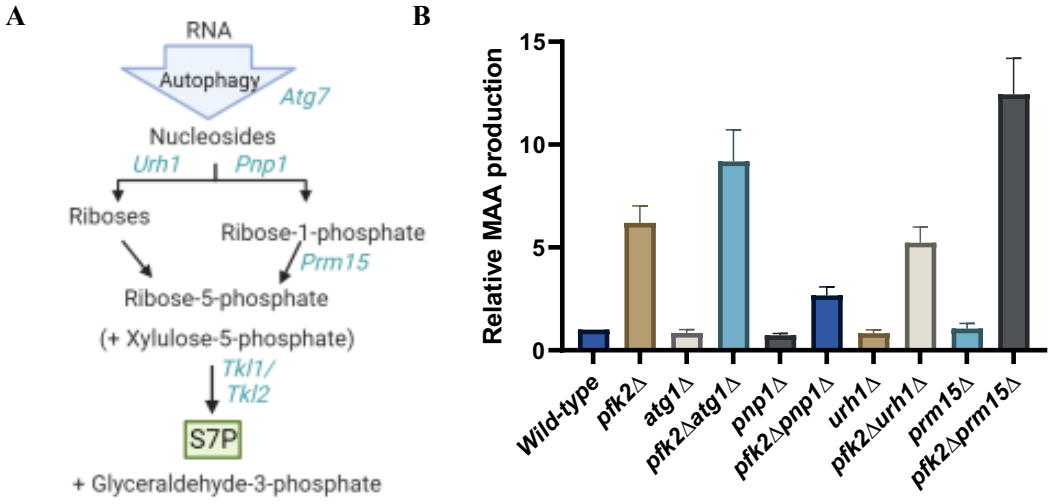

Figure S7. The nucleotide degradation and ribose salvage pathway in yeast is not responsible for the *pfk2Δ* boost in shinorine production. A) The nucleotide degradation and ribose salvage pathway in yeast. The genes *ATG7, PNP1, PRM15* and *URH1* are known to be involved in this pathway. B) Comparison of shinorine levels in the *atg1*Δ, *pnp1*Δ, *urh1*Δ and *prm15*Δ strains in the wild-type and *pfk2Δ* backgrounds.

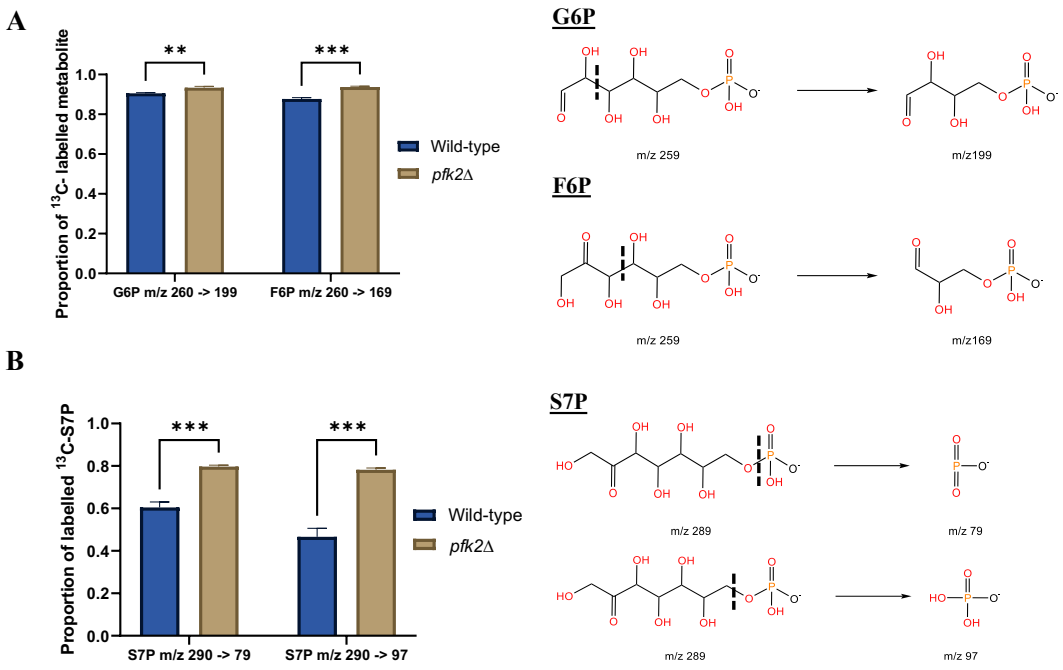

Figure S8. The fragmentation patterns of glycolytic/PPP metabolites. A) G6P and F6P fragmentation patterns. B) S7P fragmentation patterns.

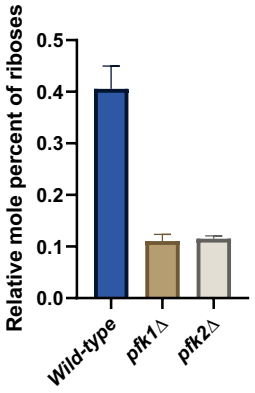

Figure S9. Comparison of the proportion of pentoses in the wild-type, *pfk1*Δ and *pfk2*Δ cells.

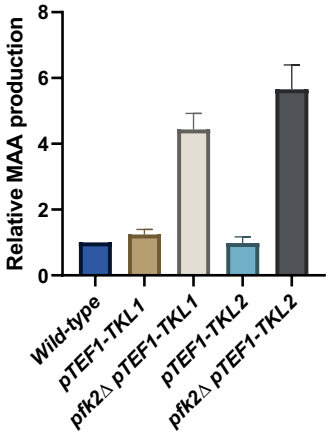

Figure S10. Changing the promoters of *TKL1* and *TKL2* to a strong constitutive promoter P_{TEF1} has limited effect on increasing MAA production.